Protein J (2014) 33:465–473
DOI 10.1007/s10930-014-9578-6

In Solution Cation-Induced Secondary and Tertiary Structure Alterations of Human Calprotectin

Mehdi Imani · Yaser Bahrami · Hossein Zarei Jaliani · Sussan Kaboudanian Ardestani

Published online: 12 September 2014

Abstract Calprotectin (CP) is widely considered to have diverse roles including growth inhibitory and apoptosis induction in a number of tumor cell lines and antimicrobial activities. As CP has been proposed to bind metal ions with high affinity, we have studied its functional and primarily its structural behavior upon Zn^{2+} and Mn^{2+} chelation solely and along with Ca^{2+}. We employed fluorescence spectroscopy and circular dichroism to determine the resulting modifications. Based upon our findings it is clear that treating CP with ions effectively weakened its natural growth inhibitory activity. Moreover, structural analysis of Zn^{2+} and Mn^{2+}-treated CPs indicated remarkable alterations in the regular secondary structures in favor of irregular structures while Zn^{2+} and Mn^{2+} treatment of CP after incubation with Ca^{2+} displayed no remarkable shifts. Tertiary structure investigation using fluorescence spectroscopy showed that CP undergoes conformational changes upon Zn^{2+} and Mn^{2+} treatment whereby Trp residues of protein is slightly exposed to the hydrophilic environment, compactness of CP is compromised, whereas in Ca^{2+}-treated CP, the tertiary structure integrity is intact upon Zn^{2+} and Mn^{2+} chelation. Interestingly, CP structural modifications upon Zn^{2+} and Mn^{2+} treatment was significantly comparable, probably due to similar radii and charges of ions. Taken all together, we have concluded that CP maintains its normal nature in Ca^{2+}-loaded state when treated with Zn^{2+} and Mn^{2+} ions. It can be suggested that Ca^{2+} not only stabilize CP structure but also helps CP to keep its structure upon metal ions chelation which is involved in host organism defense system.

Keywords Antibacterial protein · Calprotectin · Conformational alteration · Circular dichroism · Fluorescence spectroscopy

Abbreviations

CP	Calprotectin
CD	Circular dichroism
ICP-OES	Inductively coupled plasma atomic emission spectrometer
Tm	Melting temperature
ANS	8-Anilinonaphthalene-1-sulfonic acid
Zn^{2+}	Zinc
Ca^{2+}	Calcium
Mn^{2+}	Manganese

1 Introduction

Neutrophils have been recognized as the first immune cells recruited to the site of infection and engaged in defense against invading microorganisms through phagocytosis and several other processes [1]. Upon neutrophil activation, strangers could be destroyed through two distinct non-oxidative and oxidative pathways. Non-oxidative mechanism is mediated by accumulated antimicrobial agents in

M. Imani (✉) · Y. Bahrami
Department of Basic Science, Faculty of Veterinary Medicine, Urmia University, Nazloo, Urmia, Iran
e-mail: m.imani@urmia.ac.ir; mehdi_imani682@yahoo.com

H. Z. Jaliani
Department of Genetics, School of Medicine, Shahid Sadoughi University of Medical Sciences, Yazd, Iran

S. K. Ardestani
Immunology Lab, Institute of Biochemistry and Biophysics, University of Tehran, Enghelab Ave., Tehran, Iran

cytoplasmic neutrophil while in the oxidative mechanism generation of reactive oxygen species (ROS) is involved [2].

S100A8/A9 heterodimeric complex, a neutrophil cytoplasmic protein, belongs to the S100 protein family. As the complex is variously nominated [3, 4], we herein call it calprotectin (CP). It has been demonstrated that CP plays several intra- and extra-cellular roles including modulation of cell growth, antimicrobial and antifungal effects [5] and apoptosis induction in tumor cell lines [6]. It has also been documented that CP structure and function is tuned by divalent cations; particularly Zinc (Zn^{2+}), Calcium (Ca^{2+}), Manganese (Mn^{2+}) and Copper (Cu^{2+}) [6].

It has long been known that Zn^{2+} plays important roles in both adaptive and innate immunity. Moreover, Zn^{2+} is an essential ion for living organisms as it acts as a cofactor for 9 % of eukaryotic proteins [7]. Along with Zn^{2+}, Mn^{2+} is of crucial importance within bacterial homeostasis, growth, and survival. Mn^{2+} predominantly functions as a cofactor for metalloproteinases in prokaryotic cells [8]. Taking these together, Zn^{2+} and Mn^{2+} are recognized as structural cofactors for metalloproteins to keep them functioning.

It has been demonstrated that there are two Zn^{2+} and Mn^{2+} binding sites within some S100 proteins such as S100B, S100A2, S100A7 and S100A12 [9–12]. First binding site is highly homologous among S100 proteins and encompasses residues H17 and H27 in S100A8 and H91 and H95 in S100A9 [13, 14]. The second site involves residues H83 and H87 in S100A8, and H20 and D30 in S100A9 which is also similar to the canonical binding site of S100A7 and S100A12 [15, 16]. Recently, Zn^{2+} and Mn^{2+} depletion of invading microorganisms followed by controlling their growth by CP has attracted a great attention and several studies have been conducted to elucidate the respective molecular mechanisms. However, little is known about the structural and functional changes of CP upon Mn^{2+} and Zn^{2+} sequestration. Here, we first examined the effects of Zn^{2+} and Mn^{2+} on CP cytotoxic activity in human leukemic cell line MOLT4 as a model. Then, we investigated CP structural changes upon Mn^{2+} and Zn^{2+} cations sequestration solely and in the presence of Ca^{2+} with the help of in solution techniques fluorescence and circular dichroism spectroscopy.

2 Materials and Methods

2.1 Materials

Dextran T500 (31392), Dialysis tubing (D2272), SP Sepharose (S1799), Q Sepharose (Q1126), Ficoll solution (F5415), Phenylmethylsulfonyl fluoride (PMSF), Dithiothreitol (DTT), Tricin and MTT (M2128), 8-Anilinonaphthalene-1-sulfonic acid (ANS) were purchased form Sigma. All SDS-PAGE reagents and other chemicals were obtained from Merck. All buffers and solutions were prepared in double distilled deionized water.

2.2 Cell Line

MOLT4 cells were obtained from the cell bank of Pasteur Institute of Iran and used as a model to investigate purified CP function before and after Zn^{2+} and Mn^{2+} sequestration. These cells were grown in RPMI 1640 medium supplemented with 10 % FCS, 4 mM L-glutamine, 100 U penicillin, 100 µg/ml streptomycin at pH 7.4 in a humidified incubator (37 °C and 5 % CO_2).

2.3 Neutrophil Isolation

Neutrophil isolation was carried out using dextran sedimentation procedure as described previously [17]. Concisely, Fresh human blood from healthy donors was thoroughly mixed with a dextran (T-500) 6 % (w/v) solution containing 0.9 % (w/v) NaCl at 2:1 ratio, incubated for 3 h at room temperature. RBCs were then separated from leukocytes and plasma. The upper phase which contains leukocytes was collected, centrifuged and washed with PBS followed by hypotonic lysis to further eliminate residual RBCs from leukocyte populations. Subsequently, neutrophil granulocytes were isolated from other leukocytes by centrifugation on Ficoll solution at 800*g* for 30 min at 20 °C.

2.4 CP Purification

Purification of CP was performed as previously described [18]. Briefly, Neutrophils pellet was resuspended in 25 mM phosphate buffer (pH 7.4) containing 1 mM DTT, 1 M sucrose, 1 mM EDTA and 1 mM PMSF followed by sonication. After cell lysis, the soluble fraction was separated from cell debris by centrifugation. The crude neutrophil extract was then dialyzed against 25 mM Tris–HCl pH 8.0 (buffer A) and subjected to chromatography with Q Sepharose anion exchange column. Bound proteins were eluted using 0–0.5 M NaCl gradient in buffer A. Subsequently, anion-exchange eluted fractions were analyzed by tricine–sodium dodecyl sulfate–polyacrylamide gel electrophoresis (SDS-PAGE; 16.5 % gel) under reducing conditions. In the second step of purification, fractions containing CP were dialyzed against 25 mM sodium acetate pH 4.5 (buffer B) and injected into a cation exchange column (SP Sepharose). Bound proteins were eluted from the column with 0–1.0 M NaCl gradient in buffer B. Protein concentrations were determined using Bradford

reagent (Bio-Rad) and bovine serum albumin (BSA) as standard [19].

2.5 Cell Proliferation Assay

Harvested MOLT4 cells were seeded into 96-well plates (2×10^4 cell/well) in the presence of untreated-CP and Zn^{2+} and Mn^{2+}-treated CP. For examination of Zn^{2+} and Mn^{2+} reversal effect, CP preincubated with those ions and then applied into MOTL4 culture media. The inhibition rate of growth in each well was calculated as [(A570 treated cells)/(A570 control cells)] $\times$ 100 %, as described previously [20].

2.6 Quantification of Ca^{2+}, Zn^{2+} and Mn^{2+} Bound to Purified CP

Analysis of Ca^{2+}, Zn^{2+} and Mn^{2+} contents of purified CP were performed by inductively coupled plasma atomic emission spectrometer (ICP-OES). Before ICP analysis, CP was dialyzed against deionized water. The analytical wavelengths (nm) were set at 396.847, 202.548 and 259.372 for Ca^{2+}, Zn^{2+} and Mn^{2+}, respectively. The ions concentrations were calculated as ppm and were estimated for each CP molecule. We used 5 ppm of CP which corresponds to 5 μg/l. For estimation of the number of CP molecules in the solution, molecular mass of 25 kDa was considered as 1 mol of protein. For converting the ppm amounts of Ca^{2+}, Zn^{2+} and Mn^{2+} to their counts in the structure of CP, their molecular mass considered 110.98, 65.38 and 54.93 g/mol for Ca^{2+}, Zn^{2+} and Mn^{2+}, respectively.

2.7 CD Spectroscopy

CD spectra were recorded on an Aviv Spectropolarimeter (model 215, USA) to study the content of regular secondary structures of CP in the absence and presence of Ca^{2+}, Zn^{2+} and Mn^{2+}. Far UV-CD spectra were taken at 0.2 mg/ml protein concentration in 1 mm path length quartz cuvette. Protein solutions were prepared in 10 mM phosphate buffer (pH 7.4). All spectra were collected from 195 to 260 nm. The results were expressed in molar ellipticity [θ] (deg cm^2 $dmol^{-1}$) based on mean residues number of 207 and an average molecular weight of 25 kDa. The molar ellipticity was determined as $[\theta]\lambda = [100 \times (MRW) \times \theta_{obs}/(c \times l)]$, where θ_{obs} is the observed ellipticity in degrees at given wavelength, c stands for protein concentration (mg/ml) and l is the length of the light path in mm. CD software was used to predict the secondary structure [21, 22].

2.8 Fluorescence Spectroscopy

Fluorescence spectra were recorded on a Cary Eclipse fluorescence spectrophotometer (Varian, Salt Lake, Australia).

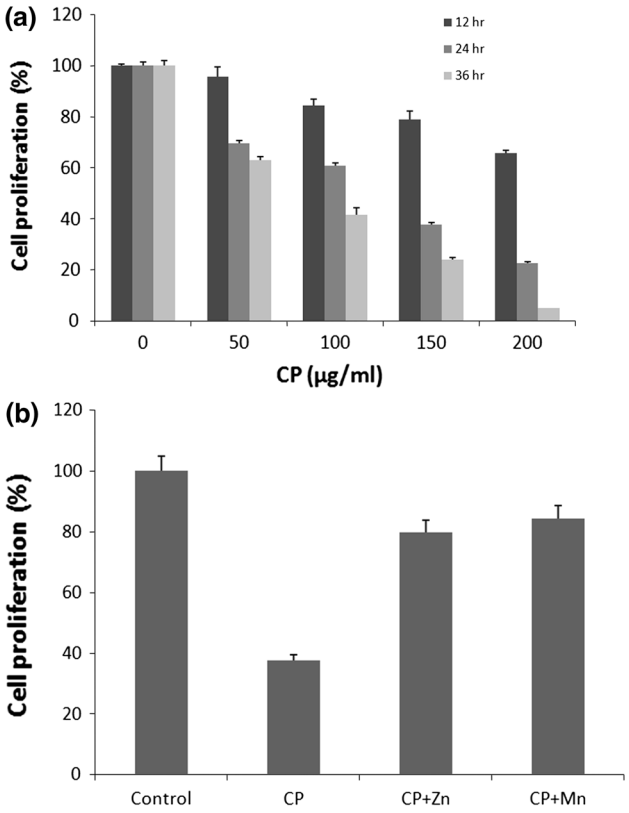

Fig. 1 **a** Cytotoxic effect of different concentrations of CP against MOLT4. MOLT4 cells were grown in a 96 well dish at the density of 2×10^4 cells/well with varying concentration of CP sample for 12, 24 and 36 h. **b** Reversal of growth inhibitory activity of CP by Zn^{2+} and Mn^{2+}. CP treated with 10 μg/ml of Zn^{2+} and Mn^{2+} was added to the MOLT4 culture media to reach the final concentration of 150 μg/ml. Untreated cells were used as controls. Cell proliferation was determined using MTT assay and is expressed as the reduction in cell number as percentage a of untreated controls. The *vertical bars* indicating standard deviation (SD) of triplicate determinations and $p < 0.05$ is considered to be significant

Intrinsic fluorescence was measured by exciting the protein solution (50 μg/ml) in the absence and presence of Ca^{2+}, Zn^{2+} and Mn^{2+} at 25 °C in 10 mM phosphate buffer (pH 7.4). The samples were excited at 290 nm wavelength and emission spectra were recorded at 300–400 nm at 25 °C. The optical bandwidths of the excitation and emission monochromators were 5 and 10 nm, respectively. For extrinsic fluorescence, 350 nm wavelength was used for ANS fluorescence. Emission spectra were recorded over the range of 400–600 nm. All measurements were performed in a 1 cm path length fluorescence cuvette.

2.9 Structural Stability of CP

Structural thermostability of CP (50 μg/ml) in the absence and presence of 2 mM Ca^{2+}, and 10 μM Zn^{2+} and 10 μM Mn^{2+} was carried out by CD spectroscopy and fluorescence spectrophotometer. The excitation wavelength for thermal

Table 1 Ca^{2+}, Zn^{2+} and Mn^{2+} content of CP analyzed by ICP-OES

Ions	ppm	Ions/CP
Ca^{2+} 396.847	0.047141	2.2
Zn^{2+} 202.548	0.019910	1.8
Mn^{2+} 259.372	0.004112	0.87

The ions concentrations in CP were calculated as ppm and estimated ions per one molecule of CP. For more details see Sect. 2

denaturation by fluorescence spectrophotometer was 290 nm which followed by recording the emission at 345 nm at each temperature. To follow thermal denaturation by CD spectroscopy, the CD signal at 222 nm was recorded.

3 Results

3.1 CP Activity

CP cytotoxic effect was investigated in MOLT4 cell line as a model using MTT assay. CP treatment of cells showed a significant growth inhibitory effect which is time and dose dependent (Fig. 1a). As depicted in Fig. 1a, CP, at concentration as low as 50 μg/ml, suppresses cell growth after 24 and 36 h. The results also demonstrated that 150 μg/ml CP induced more than 50 % of cytotoxicity after 24 h of treatment and 200 μg/ml almost killed every cultured cell.

3.2 Reversal of CP Activity Upon Zn^{2+} and Mn^{2+} Treatment

In order to clarify the divalent cation contents of purified CP, it was dialyzed against deionized water and then analyzed by ICP. Each single molecule of CP contains nearly 2.2 Ca^{2+}, 1.8 Zn^{2+} and 0.77 Mn^{2+} (Table 1). To analyze if CP cytotoxic effects can be modified by Zn^{2+} and Mn^{2+}, CP was incubated with 10 μM of either Zn^{2+} or Mn^{2+} for 30 min and then added to MOLT4 cell media. As shown in Fig. 1b, Zn^{2+} and Mn^{2+}-treated CP was unable to induce cell death compared to the untreated form. Moreover, experiments also carried out with CP preincubated with 2 mM Ca^{2+}, Zn^{2+} and Mn^{2+}. The results were the same as obtained for, Zn^{2+} and Mn^{2+}-treated CP (data not shown).

3.3 CP Secondary Structural Alteration Upon Cation Binding

To clarify if Zn^{2+} and Mn^{2+} may modify CP secondary structures, we employed Far-UV CD spectroscopy. CD is considered as an efficient tool to monitor any conformational changes in proteins under different conditions like various pH, temperature, ligand binding, and et cetera [23].

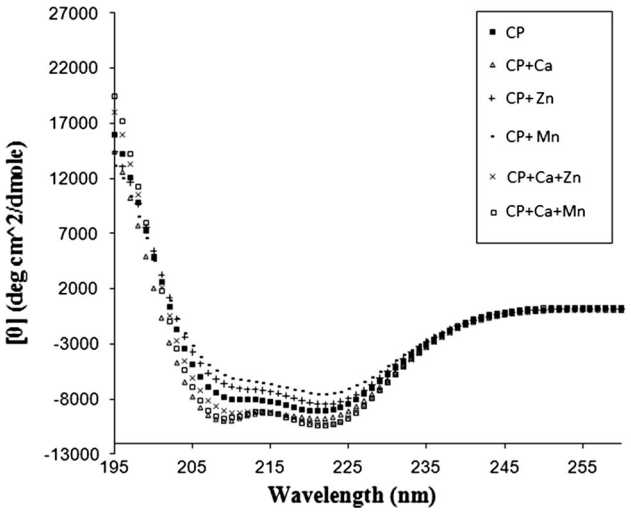

Fig. 2 Far-UV CD records of CP in the absence (*filled square*), and presence of 2 mM Ca^{2+} (*triangle*), 10 μM Zn^{2+} (*plus symbol*), 10 μM Mn^{2+} (*minus symbol*), $Ca^{2+} + Zn^{2+}$ (*times symbol*) and $Ca^{2+} + Mn^{2+}$ (*open square*). The CP concentration was 200 μg/ml in 10 mM phosphate buffer

We have used far-UV CD spectra (195–260 nm) records to determine CP secondary structural alterations in the presence of 2 mM Ca^{2+}, and 10 μM Zn^{2+} and 10 μM Mn^{2+} ions. As shown in Fig. 2, CD spectra of CP represents two negative bands at 208 and 222 nm which corresponds to α-helical structure. The data demonstrated a significant reduction in intensity of negative bands at both 208 and 222 nm upon Zn^{2+} and Mn^{2+} treatment. Conversely, CD spectra of Ca^{2+}-treated CP displayed an increase in negative bands. Similarly, incubation of Ca^{2+}-treated CP with Zn^{2+} and Mn^{2+} resulted in identical alteration (Fig. 2). Furthermore, the percentage of secondary structures was analyzed. The analysis determined that CP α-helix percentage shifts from 50–43 to 40 % in the presence of Zn^{2+} and Mn^{2+}, respectively. By contrast, incubation of CP with Ca^{2+} merely, or Ca^{2+} plus Zn^{2+} and Mn^{2+} ions notably decreased other secondary structures in favor of α-helix (Table 2).

3.4 Intrinsic and Extrinsic Fluorescence Study

We performed fluorometric measurements to analyze CP tertiary structural changes in the presence of Ca^{2+}, Zn^{2+} and Mn^{2+}. The intrinsic fluorescence emission of CP is contributed to its Trp residues only, located at sites number 54 and 88 in small and large subunits, respectively. It reflects any alterations in microenvironment of Trp residues [24, 25]. The obtained data showed a significant reduction in fluorescence intensity for Zn^{2+} and Mn^{2+}-treated CP, while for CP treated with Ca^{2+} solely and Ca^{2+} plus Zn^{2+} and Mn^{2+} an increase in fluorescence emission

Table 2 Secondary structure contents of CP. CP treated with Ca^{2+}, Zn^{2+} and Mn^{2+} and Ca^{2+} + Zn^{2+} and Mn^{2+}

Secondary structures	CP	CP + Zn	CP + Mn	CP + Ca	CP + Ca + Zn	CP + Ca + Mn
% α-Helix	50	43	40	58	58	56
% β-Structures	26	29	29	24	22	24
% Random colis	24	28	31	18	20	20

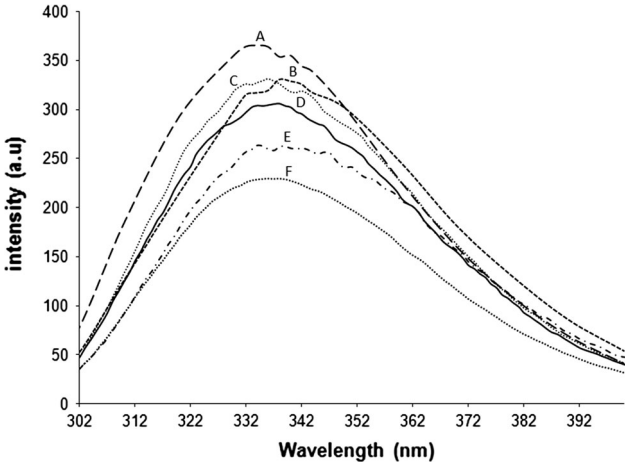

Fig. 3 Intrinsic fluorescence records of CP the absence (*D*), and presence of 2 mM Ca^{2+} (*A*), Ca^{2+} + Zn^{2+} (*B*), Ca^{2+} + Mn^{2+} (*C*), 10 μM Zn^{2+} (*E*), and 10 μM Mn^{2+} (*F*). The CP concentration was 50 μg/ml in 10 mM phosphate buffer

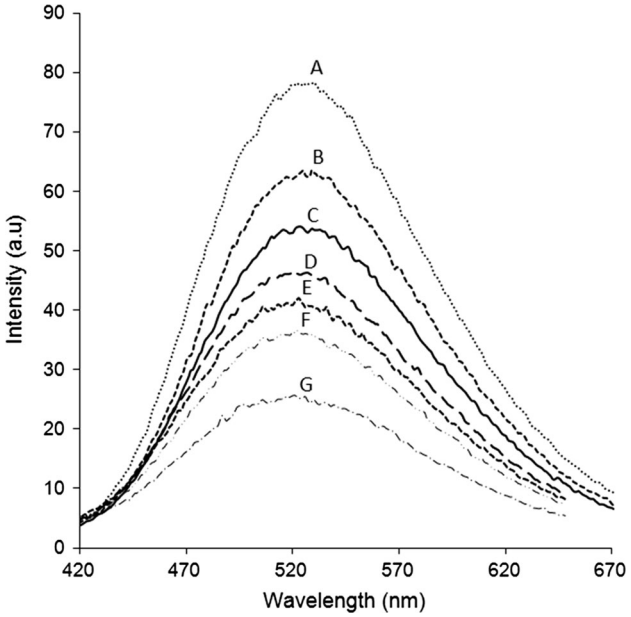

Fig. 4 ANS fluorescence records of CP in the absence (*C*), and presence of 10 μM Zn^{2+} (*A*), and 10 μM Mn^{2+} (*B*), Ca^{2+} + Zn^{2+} (*D*), Ca^{2+} + Mn^{2+} (E), and 2 mM Ca^{2+} (*F*). Spectrum G represents ANS emission. The CP concentration was 50 μg/ml in 10 mM phosphate buffer

was observed which is associate with blue shift in case of Ca^{2+}-treated CP. These results implying tertiary structural alteration in CP upon binding of cations (Fig. 3).

Following changes of ANS fluorescence upon binding to CP hydrophobic residues in the absence and presence of Ca^{2+}, Zn^{2+} and Mn^{2+} revealed when CP treated with Ca^{2+} and Ca^{2+} plus Zn^{2+} and Mn^{2+} the intensity of ANS emission reduced comparing CP ANS emission while for Zn^{2+} and Mn^{2+}-treated CP a considerable increase in fluorescence intensity was observed (Fig. 4). The reduction and increase in ANS fluorescence intensity indicate burial and accessibility of hydrophobic pockets on the protein surface to the surrounding solvent, respectively.

3.5 Structural Stability of CP

To examine CP conformational stability in the absence and presence of Ca^{2+}, Zn^{2+} and Mn^{2+}, thermal denaturation was followed by recording fluorescence emission at 345 nm upon excitation at 290 nm and CD signals at fixed wavelength 222 nm. As depicted in Fig. 5, 50 % of CP molecules were denatured at 74 °C, which is considered as Tm of the protein. Tm falls to 70 and 69 °C when treated with Zn^{2+} and Mn^{2+}, respectively while it rises to nearly 77 °C when incubated with Ca^{2+}. On the other hand, measurement of Tm for Ca^{2+}-treated CP after adding Zn^{2+} and Mn^{2+} also represented a rise in Tm relative to CP itself. Additionally, investigation of CP secondary structure Tm by CD at the above-mentioned conditions showed slight changes in Tm of cations-treated CP comparing intact CP (Table 3).

4 Discussion

Several studies have shown that two Zn^{2+} binding sites exist within some S100 proteins such as S100B, S100A2, S100A7 and S100A12 [9–12]. Metal binding regulates their interactions with target molecules such as RAGE, tau and others, implying protein conformations alteration for specific function [11, 26]. CP is an essential antibacterial factor that plays a key role through chelation of Zn^{2+} and Mn^{2+} ions in nutritional immunity [13, 27]. Cytostatic function of CP against various cell types is considered to be most likely due to its ability to bind and chelate divalent metal ions including Zn^{2+}, Mn^{2+} and Cu^{2+} [6, 28, 29].

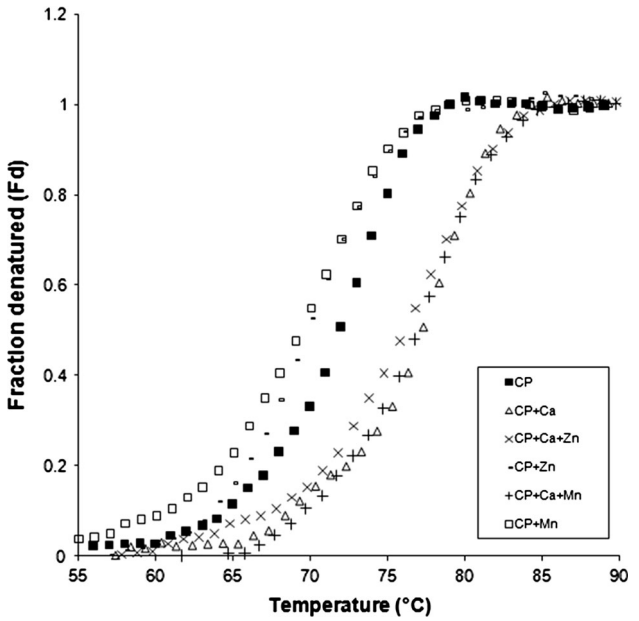

Fig. 5 The thermal denaturation profiles for the CP in the absence (*filled square*), and presence of 2 mM Ca^{2+} (*triangle*), 10 μM Zn^{2+} (*minus symbol*), 10 μM Mn^{2+} (*open square*), $Ca^{2+} + Zn^{2+}$ (*times symbol*) and $Ca^{2+} + Mn^{2+}$ (*plus symbol*). The CP concentration was 50 μg/ml in 10 mM phosphate buffer. Fraction of protein denatured is plotted against temperature. Denaturation process was followed by recording emission at 345 nm, and the apparent fraction of denatured protein. Fd was calculated as described in the text

Table 3 Melting temperature of CP

Protein	Tm of tertiary structure (°C)	Tm of secondary structure (°C)
CP	74 ± 1	73 ± 0.53
CP + Ca^{2+}	77 ± 0.96	78 ± 1.33
CP + Zn^{2+}	70 ± 1.45	73 ± 0.87
CP + Mn^{2+}	69 ± 0.91	71 ± 1.04
CP + Ca^{2+} + Zn^{2+}	78 ± 1.24	76 ± 0.68
CP + Ca^{2+} + Mn^{2+}	77 ± 1.09	76 ± 1.09

CP treated with Ca^{2+}, Zn^{2+} and Mn^{2+} and $Ca^{2+} + Zn^{2+}$ and Mn^{2+} obtained by CD and fluorescence spectroscopy

Despite efforts to reveal the molecular mechanism of CP divalent ion chelation and subsequent biological function in host defense, little is known about this process [27, 30]. Nonetheless, full structural changes of CP upon Ca^{2+}, Zn^{2+} and Mn^{2+} chelation still remain unclear. To address this, we focused on the study of CP secondary and tertiary structural changes using spectroscopy techniques. Prior to any investigation, analyzing and quantification of ions content of CP by ICP-OES technique is carried out. With the help of ICP-OES, the amount of Ca^{2+}, Zn^{2+} and Mn^{2+} was calculated to be approximately two Ca^{2+} and Zn^{2+} and one Mn^{2+} per heterodimer of CP, which is compatible with the results of isothermal titration calorimetry (ITC) experiments conducted by Chazin's group [13]. Distinct Ca^{2+} and Zn^{2+}-binding sites have been demonstrated for CP. Each monomer of CP composed of 2 EF-hand motives: N-terminal non-canonical EF-hand Ca^{2+}-binding loop (site I), represents diverse sequences are not always occupied with Ca^{2+}. C-terminal canonical EF-hand Ca^{2+}-binding loop (site II), shares consensus sequences among S100 protein family, displays high affinity for Ca^{2+} and is always occupied with Ca^{2+} both in small and large subunits [14, 31]. Moreover, each monomer of CP shares 2 aminoacids to form 2 Zn^{2+} binding sites at the heterodimer interface called site I (His3Asp) and site II (His4). The site I constitutes metal binding sites in other S100 proteins such as S100A7 and S100A12 and some metalloproteins [15, 16]. ICP data indicated that purified CP still maintain 2 Ca^{2+} and 2 Zn^{2+} in its structure during purification process. After estimating the Ca^{2+}, Zn^{2+} and Mn^{2+} content of CP, in order to investigate the activity of purified CP, various concentrations of CP were used against MOLT4 cell line as a model. As shown in Fig. 1a, CP at concentration 150 μg/ml has significant inhibitory effect on cell growth and over 50 % of cell growth has been inhibited. To address whether cytotoxic activity arisen from CP, MOLT4 cells were exposed to Zn^{2+} and Mn^{2+}-treated CP. As clearly demonstrated in Fig. 1b, the CP-mediated cytotoxic activity has been abolished when CP pretreated with Zn^{2+} and Mn^{2+} which implies inability of metal-loaded CP in Zn^{2+} and Mn^{2+} chelation so that cells escape from Zn^{2+} and Mn^{2+} deprivation. The available evidence indicate that CP inhibit cancer cell growth most likely by apoptosis and/or metal ions chelation [6, 29]. Pretreatment of CP with either Ca^{2+} or Ca^{2+} plus Zn^{2+} and Mn^{2+} ions lead to the same cytotoxic effects which can be interpreted by the fact that even though purified CP is not occupied with all 4 Ca^{2+} ions but it exert its effect most probably by using and capturing Ca^{2+} ions from cell culture media. To shed light on any structural alteration by Ca^{2+}, Zn^{2+} and Mn^{2+}, we tried to examine CP structure using spectroscopic techniques. To determine to what extent Ca^{2+}, Zn^{2+} and Mn^{2+} are able to affect the secondary structure of the CP, structural studies were performed by means of circular dichroism spectroscopic analysis. Studies have shown that CD spectra of CP encompasses two remarkable negative bands at 208 and 222 nm which point out the existence of α-helical structures in CP [18]. From the CD spectra and secondary structure content of CP in the presence of Zn^{2+} and Mn^{2+}, it is noticeable that both ions significantly decrease the negative value of $[\theta]_{222}$, reducing α-helix content which is associated with increasing the content of β-structures and random coils. On the other hand, structural conformation of CP undergoes a noticeable changes in the presence of Zn^{2+} and Mn^{2+}. Furthermore, CD signals of

CP in the presence of Ca^{2+}, and Ca^{2+} plus Zn^{2+} and Mn^{2+} were recorded. The results showed that Ca^{2+} affects secondary structure of CP in favor of ordered α-helix structure by reducing random coiled structure of CP. In fact, it can be suggested that, excess amount of Ca^{2+} causes CP to oligomerize into heterotetrameric form. Moreover, the CD records of Ca^{2+}-treated CP in the presence of Zn^{2+} and Mn^{2+} ions suggested highly similar profile comparing to that of Ca^{2+}-treated CP. Therefore, it implies that both ions have no effects on the secondary structures of Ca^{2+}-preloaded CP.

Damo et al. [27] has recently reported the detailed Mn^{2+} binding site on the CP heterodimer, in which two additional histidines of the S100A9 C-terminal loop are also involved in Mn^{2+} sequestration. They highlighted the more stable structure of this loop, so that the detailed structure of loop has become visible in Mn^{2+}-bound CP crystal (PDB code: 4GGF) in contrast with the Mn^{2+}-free CP crystal structure (PDB code: 1XK4). They also concluded that binding of Mn^{2+} does not change the overall structure of CP but probably at the very C-terminal loop of large subunit S100A9. Besides, Nolan group has thoroughly analyzed Zn^{2+} and Mn^{2+} coordination at their respective binding sites in connection to Ca^{2+} at molecular level [32, 33].

Even though, increase in negative ellipticity mostly regarded as increase in helical content of a protein but it can also be considered that ellipticity changes can be attributed to the features other than that. In the current study, decrease or increase in negative ellipticity of CP as a result of ions treatment not only may be attributed to the alteration in helical content but also can be related to the spatial orientation of helices as was already evident for troponin C [34, 35] Moreover, oligomerization of a protein can give rise to a change in negative ellipticity. Biophysical studies of CP have shown that Zn^{2+} triggers tetramerization of CP by binding to Zn^{2+}-specific binding sites rather than by interaction with Ca^{2+}-specific EF-hands [36]. Consistent with that, our data showed that incubation of CP with Zn^{2+} and Mn^{2+} lead to decrease in negative ellipticity may be indicative of higher ordered structure of CP, as well.

Several changes in the conformation of protein molecules due to ligand binding can be monitored by fluorometric techniques which are also commonly used in monitoring the minor changes in the conformation of protein molecules due to environmental condition fluctuation, amino acid mutations and etcetera. The alteration in the intrinsic fluorescence emission spectra reflects the conformational changes of the protein structure that originate from the microenvironment changes of the Trp residues available in the small and large subunits of CP. By exciting CP at the wavelength of 290 nm and recording fluorescence emission around 345 nm, changes in the microenvironment of the tryptophan residues can be obtained. To monitor this, measurement of fluorescence emission of CP in the presence of Ca^{2+} and Ca^{2+} plus Zn^{2+} and Mn^{2+} at 25 °C was conducted. As it is evident in Fig. 3, reduction of fluorescence emission at 345 nm was observed for Zn^{2+} and Mn^{2+} -treated CP. The quenching of Trp 54 or Trp 88 fluorescence suggests that divalent ions effectively influence the conformation of the CP which in turns expose the Trp(s) to the hydrophilic environment when CP is not fully loaded by Ca^{2+}. By contrast, fluorescence emission of CP not only increased in the presence of Ca^{2+} but also a significant blue shift is noticed. When blue shifted emission is attained it implies that Trp enters more hydrophobic environment. These spectral changes point to the fact that CP tertiary structure changes due to Ca^{2+} binding. Analyzing tertiary structure of Ca^{2+}-treated CP in the presence of Zn^{2+} and Mn^{2+} ions also indicated nearly identical spectra which represent that Zn^{2+} and Mn^{2+} has no significant effects on Ca^{2+}-preloaded CP.

ANS, an extrinsic fluorophore which contains both hydrophilic and hydrophobic regions is widely used to study protein dynamic changes. Once it binds to the hydrophobic region of the protein the fluorescence emission intensity enhances [37]. Therefore, it is useful in investigation of CP conformational changes, ANS fluorescence emission of CP pretreated with Ca^{2+}, Zn^{2+} and Mn^{2+} at 25 °C are depicted in Fig. 4. From the results, one can conclude the movement of the hydrophobic patches of CP into hydrophilic (solvent) environment in the presence of Zn^{2+} and Mn^{2+} which indicates them more accessible to the ANS binding. In other words, Zn^{2+} and Mn^{2+} induce a relatively more loose structure or compromise the compactness of tertiary structure when CP is partially occupied with Ca^{2+}. Furthermore, studies indicated that dimerization plane of S100 proteins composed of conserved hydrophobic residues and underwent conformational change under different conditions inferred from the emission increase of ANS [38]. Based on our results it can be inferred that at least Zn^{2+} and Mn^{2+} exerts a conformational changes on CP structure in the absence of Ca^{2+}.

To clarify the effect of Ca^{2+}, Zn^{2+} and Mn^{2+} on the structure of CP with more details, we also examined the conformational stability of protein. Analysis of thermal denaturation process was carried out by both CD and fluorescence spectroscopy. Examination tertiary structure Tm of CP by fluorescence spectroscopy indicated a Tm of 74 °C. Whereas Tm of CP shifted to 77 °C when CP incubated with 2 mM Ca^{2+} (Fig. 5; Table 3). Estimation of secondary structure Tm by CD spectroscopy displayed almost the same Tm. These increase in conformational stability of CP in the presence of excess amount of Ca^{2+} agree with results of Nolan group in which they showed that Tm of CP increases 20 and 13 °C obtained by CD spectroscopy and differential scanning calorimetry, respectively [32]. Surprisingly, in the

absence of Ca^{2+} and presence of Zn^{2+} and Mn^{2+}, Tm of CP reduced to almost 70 °C which represents that both ions have unfavorable effects on the thermal stability of the CP (Table 3). It can be suggested that as far as CP is not fully occupied with Ca^{2+}, both Zn^{2+} and Mn^{2+} not only alter its conformation but also influence its thermal stability and make it susceptible to changes in the environmental conditions. Moreover, several studies have demonstrated that the mechanism by which CP inhibit bacterial growth is dependent on its metal chelation ability. Kehl-Fie et al. created CP mutants lacking binding sites for Zn^{2+} and Mn^{2+}. They also demonstrated that CP reduces both the activity of Mn^{2+}-dependent superoxide dismutases (SOD) and other Mn^{2+}-dependent mechanisms of superoxide defense in *S. aureus* which indicative of high cation-binding capacity of CP. Inactivating of these defense systems in *S. aureus* probably made it more sensitive to neutrophil-mediated killing mechanisms [13]. The spectroscopy results presented here indicates that CP undergoes conformational changes upon chelation of either Zn^{2+} or Mn^{2+} once amount of Ca^{2+} is insufficient. Fortunately, since Ca^{2+} concentration of extracellular media is in millimolar range, neutrophil-secreted CP basically contains sufficient amount of Ca^{2+} to preserve its stable structure even after chelation of Zn^{2+} or Mn^{2+}. Mass spectrometric investigations have demonstrated that Zn^{2+} ions are able to induce heterotetramer CP. Zn^{2+} ions accomplish this not only by binding to specific Zn^{2+} binding sites but they probably interact non-specifically with EF-hand motives. However, Zn^{2+} ions are replaced in excess amount of Ca^{2+} [36]. Indeed, CP experience different conformation in the absence of essential amount of Ca^{2+} if it is secreted out of neutrophils. Zn^{2+}-induced conformation lead to dysfunctional properties of CP so that its arachidonic acid binding property abolished. Investigations have provided evidence that this effect was due to conformational changes which affect arachidonic acid binding pocket within CP [39]. Taken together, it can be concluded that insufficiency of Ca^{2+} give rise to a CP with less proper and stable structure and availability of Ca^{2+} is prerequisite for its physiological functions.

Acknowledgments Authors would like to express their deepest gratitude to Dr. Saeed Yadranji Aghdam and Dr. Kourosh Shahpasand for their valuable comments to improve the quality of the paper. We also gratefully acknowledge the support from research council of Urmia University.

Conflict of interest All the authors declare no conflict of interest.

References

1. Mollinedo F, Borregaard N, Boxer LA (1999) Novel trends in neutrophil structure, function and development. Immunol Today 20(12):535–537. doi:10.1016/S0167-5699(99)01500-5
2. Vethanayagam RR, Almyroudis NG, Grimm MJ, Lewandowski DC, Pham CTN, Blackwell TS, Petraitiene R, Petraitis V, Walsh TJ, Urban CF, Segal BH (2011) Role of NADPH oxidase versus neutrophil proteases in antimicrobial host defense. PLoS One 6(12):e28149
3. Odink K, Cerletti N, Bruggen J, Clerc RG, Tarcsay L, Zwadlo G, Gerhards G, Schlegel R, Sorg C (1987) Two calcium-binding proteins in infiltrate macrophages of rheumatoid arthritis. Nature 330(6143):80–82
4. Johne B, Fagerhol MK, Lyberg T, Prydz H, Brandtzaeg P, Naess-Andresen CF, Dale I (1997) Functional and clinical aspects of the myelomonocyte protein calprotectin. Mol Pathol 50(3):113–123
5. Sohnle PG, Hahn BL, Santhanagopalan V (1996) Inhibition of candida albicans growth by calprotectin in the absence of direct contact with the organisms. J Infect Dis 174(6):1369–1371. doi:10.1093/infdis/174.6.1369
6. Yui S, Mikami M, Tsurumaki K, Yamazaki M (1997) Growth-inhibitory and apoptosis-inducing activities of calprotectin derived from inflammatory exudate cells on normal fibroblasts: regulation by metal ions. J Leukoc Biol 61(1):50–57
7. Andreini C, Bertini I, Rosato A (2009) Metalloproteomes: a bioinformatic approach. Acc Chem Res 42(10):1471–1479. doi:10.1021/ar900015x
8. Jakubovics NS, Jenkinson HF (2001) Out of the iron age: new insights into the critical role of manganese homeostasis in bacteria. Microbiology 147(7):1709–1718
9. Wilder PT, Varney KM, Weiss MB, Gitti RK, Weber DJ (2005) Solution structure of zinc- and calcium-bound rat S100B as determined by nuclear magnetic resonance spectroscopy. Biochemistry 44(15):5690–5702
10. Brodersen DE, Nyborg J, Kjeldgaard M (1999) Zinc-binding site of an S100 protein revealed. Two crystal structures of Ca^{2+}-bound human psoriasin (S100A7) in the Zn^{2+}-loaded and Zn^{2+}-free states. Biochemistry 38(6):1695–1704
11. Moroz OV, Burkitt W, Wittkowski H, He W, Ianoul A, Novitskaya V, Xie J, Polyakova O, Lednev IK, Shekhtman A (2009) Both Ca^{2+} and Zn^{2+} are essential for S100A12 protein oligomerization and function. BMC Biochem 10(1):11
12. Ostendorp T, Diez J, Heizmann CW, Fritz G (2011) The crystal structures of human S100B in the zinc- and calcium-loaded state at three pH values reveal zinc ligand swapping. Biochim Biophys Acta (BBA) Mol Cell Res 1813(5):1083–1091
13. Kehl-Fie Thomas E, Chitayat S, Hood MI, Damo S, Restrepo N, Garcia C, Munro Kim A, Chazin Walter J, Skaar Eric P (2011) Nutrient metal sequestration by calprotectin inhibits bacterial superoxide defense, enhancing neutrophil killing of *Staphylococcus aureus*. Cell Host Microbe 10(2):158–164
14. Korndörfer IP, Brueckner F, Skerra A (2007) The crystal structure of the human (S100A8/S100A9)2 heterotetramer, calprotectin, illustrates how conformational changes of interacting α-helices can determine specific association of two EF-hand proteins. J Mol Biol 370(5):887–898. doi:10.1016/j.jmb.2007.04.065
15. Moroz OV, Blagova EV, Wilkinson AJ, Wilson KS, Bronstein IB (2009) The crystal structures of human S100A12 in apo form and in complex with zinc: new insights into S100A12 oligomerisation. J Mol Biol 391(3):536–551. doi:10.1016/j.jmb.2009.06.004
16. Brodersen DE, Nyborg J, Kjeldgaard M (1999) Zinc-binding site of an S100 protein revealed. Two crystal structures of Ca^{2+}-bound human psoriasin (S100A7) in the Zn^{2+}-loaded and Zn^{2+}-free states. Biochemistry 38(6):1695–1704. doi:10.1021/bi982483d
17. Skoog WA, Beck WS (1956) Studies on the fibrinogen, dextran and phytohemagglutinin methods of isolating leukocytes. Blood 11(5):436–454
18. Yousefi R, Imani M, Ardestani SK, Saboury AA, Gheibi N, Ranjbar B (2007) Human calprotectin: effect of calcium and zinc

on its secondary and tertiary structures, and role of pH in its thermal stability. Acta Biochim Biophys Sin 39(10):795–802. doi:10.1111/j.1745-7270.2007.00343.x
19. Bradford MM (1976) A rapid and sensitive method for the quantitation of microgram quantities of protein utilizing the principle of protein-dye binding. Anal Biochem 72(1–2):248–254. doi:10.1016/0003-2697(76)90527-3
20. Mosmann T (1983) Rapid colorimetric assay for cellular growth and survival: application to proliferation and cytotoxicity assays. J Immunol Methods 65(1–2):55–63. doi:10.1016/0022-1759(83)90303-4
21. Schippers PH, Dekkers HPJM (1981) Direct determination of absolute circular dichroism data and calibration of commercial instruments. Anal Chem 53(6):778–782. doi:10.1021/ac00229a008
22. Manavalan P, Johnson WC Jr (1987) Variable selection method improves the prediction of protein secondary structure from circular dichroism spectra. Anal Biochem 167(1):76–85. doi:10.1016/0003-2697(87)90135-7
23. Kelly SMPN (2000) The use of circular dichroism in the investigation of protein structure and function. Curr Protein Pept Sci 1(4):349–384
24. Kerkhoff C, Klempt M, Sorg C (1998) Novel insights into structure and function of MRP8 (S100A8) and MRP14 (S100A9). Biochim Biophys Acta (BBA) Mol Cell Res 1448(2):200–211. doi:10.1016/S0167-4889(98)00144-X
25. Hessian PA, Edgeworth J, Hogg N (1993) MRP-8 and MRP-14, two abundant Ca(2+)-binding proteins of neutrophils and monocytes. J Leukoc Biol 53(2):197–204
26. Yu WH, Fraser PE (2001) S100β interaction with tau is promoted by zinc and inhibited by hyperphosphorylation in Alzheimer's disease. J Neurosci 21(7):2240–2246
27. Damo SM, Kehl-Fie TE, Sugitani N, Holt ME, Rathi S, Murphy WJ, Zhang Y, Betz C, Hench L, Fritz G, Skaar EP, Chazin WJ (2013) Molecular basis for manganese sequestration by calprotectin and roles in the innate immune response to invading bacterial pathogens. Proc Natl Acad Sci 110(10):3841–3846. doi:10.1073/pnas.1220341110
28. Yui S, Nakatani Y, Mikami M (2003) Calprotectin (S100A8/S100A9), an inflammatory protein complex from neutrophils with a broad apoptosis-inducing activity. Biolog Pharm Bull 26(6):753–760
29. Yui S, Nakatani Y, Hunter MJ, Chazin WJ, Yamazaki M (2002) Implication of extracellular zinc exclusion by recombinant human calprotectin (MRP8 and MRP14) from target cells in its apoptosis-inducing activity. Med Inflamm 11(3):165–172. doi:10.1080/09622935020138208
30. Corbin BD, Seeley EH, Raab A, Feldmann J, Miller MR, Torres VJ, Anderson KL, Dattilo BM, Dunman PM, Gerads R, Caprioli RM, Nacken W, Chazin WJ, Skaar EP (2008) Metal chelation and inhibition of bacterial growth in tissue abscesses. Science 319(5865):962–965. doi:10.1126/science.1152449
31. Gifford JL, Walsh MP, Vogel HJ (2007) Structures and metal-ion-binding properties of the Ca^{2+}-binding helix–loop–helix EF-hand motifs. Biochem J 405(2):199–221
32. Brophy MB, Hayden JA, Nolan EM (2012) Calcium ion gradients modulate the zinc affinity and antibacterial activity of human calprotectin. J Am Chem Soc 134(43):18089–18100. doi:10.1021/ja307974e
33. Hayden JA, Brophy MB, Cunden LS, Nolan EM (2012) High-affinity manganese coordination by human calprotectin is calcium-dependent and requires the histidine-rich site formed at the dimer interface. J Am Chem Soc 135(2):775–787. doi:10.1021/ja3096416
34. Slupsky CM, Smillie LB, Sykes BD, Reinach FC (1995) Solution secondary structure of calcium-saturated troponin C monomer determined by multidimensional heteronuclear NMR spectroscopy. Protein Sci 4(7):1279–1290
35. Gagné SM, Tsuda S, Li MX, Chandra M, Smillie LB, Sykes BD (1994) Quantification of the calcium-induced secondary structural changes in the regulatory domain of troponin-C. Protein Sci 3(11):1961–1974. doi:10.1002/pro.5560031108
36. Vogl T, Leukert N, Barczyk K, Strupat K, Roth J (2006) Biophysical characterization of S100A8 and S100A9 in the absence and presence of bivalent cations. Biochim Biophys Acta (BBA) Mol Cell Res 1763(11):1298–1306. doi:10.1016/j.bbamcr.2006.08.028
37. Matulis D, Baumann CG, Bloomfield VA, Lovrien RE (1999) 1-Anilino-8-naphthalene sulfonate as a protein conformational tightening agent. Biopolymers 49(6):451–458. doi:10.1002/(sici)1097-0282(199905)49:6<451:aid-bip3>3.0.co;2-6
38. Carvalho SB, Botelho HM, Leal SS, Cardoso I, Fritz G, Gomes CM (2013) Intrinsically disordered and aggregation prone regions underlie β-aggregation in S100 proteins. PLoS One 8(10):e76629
39. Kerkhoff C, Vogl T, Nacken W, Sopalla C, Sorg C (1999) Zinc binding reverses the calcium-induced arachidonic acid-binding capacity of the S100A8/A9 protein complex. FEBS Lett 460(1):134–138. doi:10.1016/S0014-5793(99)01322-8